

PAPER • OPEN ACCESS

## Evaluation of melting behaviour of Nickel, Titanium, and NiTi alloy using EAM and MEAM type potential

To cite this article: R Arifin *et al* 2019 *J. Phys.: Conf. Ser.* **1171** 012035

View the [article online](#) for updates and enhancements.

### Recent citations

- [Pressure dependence of the structure of liquid NiTi: a molecular dynamics study](#)  
Rizal Arifin *et al*



**IOP | ebooks™**

Bringing you innovative digital publishing with leading voices to create your essential collection of books in STEM research.

Start exploring the collection - download the first chapter of every title for free.

# Evaluation of melting behaviour of Nickel, Titanium, and NiTi alloy using EAM and MEAM type potential

R Arifin<sup>1</sup>, M Malyadi<sup>1</sup>, Munaji<sup>1</sup>, G A Buntoro<sup>1</sup>, and Darminto<sup>2</sup>

<sup>1</sup>Department of Mechanical Engineering, Universitas Muhammadiyah Ponorogo, Jl. Budi Utomo No. 10, Ponorogo 63471 Indonesia

<sup>2</sup>Department of Physics, Institut Teknologi Sepuluh Nopember, Kampus ITS Sukolilo, Surabaya 60111 Indonesia

E-mail: rarifin@umpo.ac.id

**Abstract.** The atomic level study of NiTi alloy at high temperature is very important to understand the mechanism of NiTi fabrication, in partial the process during the hot working. In the atomic investigation using molecular dynamics simulation, the use of the interatomic potential greatly affects the results. Therefore, the suitability of the interatomic potential applied in some specific condition has to be examined. In our previous work, we have tested the performance of EAM and MEAM potential to reproduce the lattice constant of NiTi alloy. Our previous results have shown that the MEAM potential work better than the EAM potential. In this research, we further investigate the performance of EAM and MEAM type potential to describe the melting behavior of nickel, titanium, and NiTi alloy. We find from the current result that the accuracy of the MEAM potential is better than EAM potential in high temperature MD simulations.

## 1. Introduction

Nickel and titanium are two kinds of precious metals. These metals are widely used with other metal in many applications. Nickel and titanium can also be used together as the alloy metal which is also called nitinol. NiTi alloy is the interesting material exhibiting shape memory effect (SME). This material can return to its original structure at specific temperature after it is deformed into other shapes. The structural change of the NiTi alloy is very sensitive to the composition of nickel and titanium atoms and the heat treatment. By these properties, NiTi is categorized as the shape memory alloy (SMA) [1,2]. NiTi alloy has some valuable properties such as high electrical resistivity, corrosion resistance, highly biocompatible, water resistance and many others. Therefore this material are widely used as the biomaterial, medical devices, and military devices [3-5].

Although NiTi alloy has many potential applications, however the fabrication process of this material is not easy. This problem may cause the increase of the NiTi alloy price. The theoretical study of the atomic behavior of NiTi alloy will guide the researcher and the industry to understand the mechanism of its formation during the fabrication. The fabrication process of NiTi alloy is done both in the high and the low temperature conditions. To the best to our knowledge, there are only few molecular dynamics (MD) simulation works investigating of NiTi behavior at high temperatures [6-8]. However, those reported papers did not concern with the composition of atomic structure of nickel, titanium, and NiTi alloy in their melting temperatures. It is known that the interatomic potential plays a crucial role in MD simulations. Therefore, the interatomic potential has to be evaluated before it is used to obtain



the result in MD simulations. Recently, two interatomic potentials are developed for NiTi alloys, *i.e.* standard embedded-atom-method (EAM) potential by Zhou et al. [9] and modified EAM (MEAM) potential by Ko et al. [10]. This study aims to investigate the usability of these potentials in high temperature simulation condition. We determine the performance of these potential based on the accuracy of each potential in obtaining the melting temperature of the systems.

## 2. Methods

In this section, we present the detail of the interatomic potentials employed in our MD simulation. The procedures for the calculation and the analysis of the results are also explained thoroughly.

### 2.1. Interatomic potentials

Two types of the interatomic potentials, *i.e.*, the EAM [11,12] and the MEAM [13] are used to describe the interactions between atoms in the simulation system. The formalism of the total energy in the EAM type potential is written as [10]

$$E = \sum_i \left[ F_i(\bar{\rho}_i) + \frac{1}{2} \sum_{j(\neq i)} \phi_{ij}(R_{ij}) \right], \quad (1)$$

where  $F_i$  is the embedding energy as the function of the average electron density  $\bar{\rho}_i$  and  $\phi_{ij}$  is the pair potential between atoms  $i$  and  $j$  separated by a distance  $R_{ij}$ . The electron density of atom  $i$  is obtained from the sum of the electron density of the neighbouring atom  $j$ ,

$$\rho_i = \sum_{j \neq i} \rho_j(R_{ij}) \quad (2)$$

In the MEAM potential, the angular terms are included in the formulation of the total atomic electron density to account the directional character of bonding. The total atomic electron density is obtained from the combination of partial electron density from different angular contribution with weighting factor  $t^{(h)}$  in which  $h = 1 - 3$ . Each partial electron density is the function of atomic configuration and the atomic electron density  $\rho^{a(h)}$  ( $h = 0 - 4$ ),

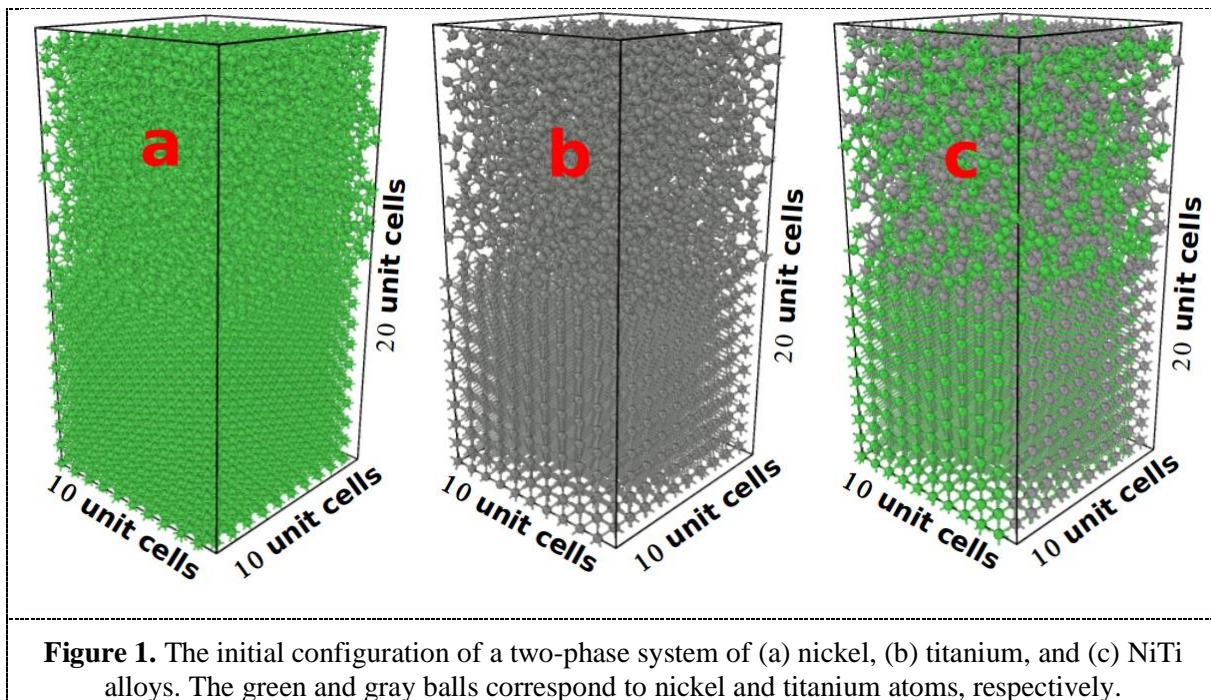
$$\rho^{a(h)}(R) = \rho_0 \exp[-\beta^{(h)}(R/r_e - 1)] \quad (3)$$

where  $\rho_0$ ,  $\beta^{(h)}$ , and  $r_e$  are atomic electron density scaling factor, decay lengths, and the nearest-neighbor distance in the equilibrium reference structure, respectively.

The parameters of the EAM and the MEAM potential are normally fitted from the results of the *ab initio* calculations. In this simulation, we choose the EAM and MEAM parameters for NiTi system generated by Zhou et al. [9] and Ko et al. [10], respectively.

### 2.2. Simulation procedure and results analysis

All the MD simulations are carried out using the Large-scale Atomic/Molecular Massively Parallel Simulator (LAMMPS) package [14]. At first, we generate the atomic configuration of nickel, titanium, and NiTi system in fcc, bcc, and b2 crystal structure, respectively. The dimensions of the supercell is  $10 \times 10 \times 20$  unit cells along the  $x$ -,  $y$ -, and  $z$ -directions. Figure 1 shows the initial structure of the nickel, the titanium, and the NiTi alloy systems.



The constant temperatures and the pressure are achieved in this simulation using the NPT Nosé-Hoover procedure [15,16]. The Verlet algorithm is used to solve the equations of motion numerically. The timestep of our MD simulation is 1 fs. Each MD simulation is performed for 100 ps (100.000 MD steps). The atomic configurations are visualized using the Ovito software [17]. In this simulation, we calculate the melting temperature  $T_m$  of nickel, titanium, and NiTi alloy using a method, so called two-phase approach which exhibit the good accuracy in our previous simulation of aluminium system [18]. Its initial configuration consists of two different structures, *i.e.*, crystal and liquids. The atoms located in the upper half of the system are melted, while the lower half atoms are maintained in the crystal structure.

The density profile analysis is used to observe the spatial structure of the system [19]. The atomic structures in the system are identified by Bond-angle analysis [20].

### 3. Results and Discussion

In this section, we compare the melting temperature of the nickel, titanium, and NiTi alloy estimated from two-phase approach by employing EAM [9] and MEAM [10] potentials in the MD simulations. Further, we also report our results of the atomic structure composition when the systems reach the melting temperatures.

#### 3.1. Melting temperatures of nickel, titanium, and NiTi alloys

One of the methods widely used to estimate the melting temperature of the metal system in the MD simulation is two-phase approach. This method is known for its accuracy compared with other methods. In our previous MD simulation of aluminium system, it has been shown that the result from two-phase approach is better than that one from one-phase approach [18].

The MEAM potential has been reported to outperform the EAM potential at low temperature simulations of NiTi alloy [10, 21]. The MEAM potential by Ko et al. can reproduce the more accurate lattice parameter of NiTi alloy than the EAM potential by Zhou et al. [21]. The martensitic transformation of NiTi alloy can also be described accurately using MEAM potential [10]. However, the result can be different in other simulation conditions. Therefore, we currently examine the performance of MEAM and EAM potentials for nickel, titanium, and NiTi alloy at high-temperature MD simulation. The higher accuracy of the calculated melting temperature indicates the better performance of the potential at high temperature.

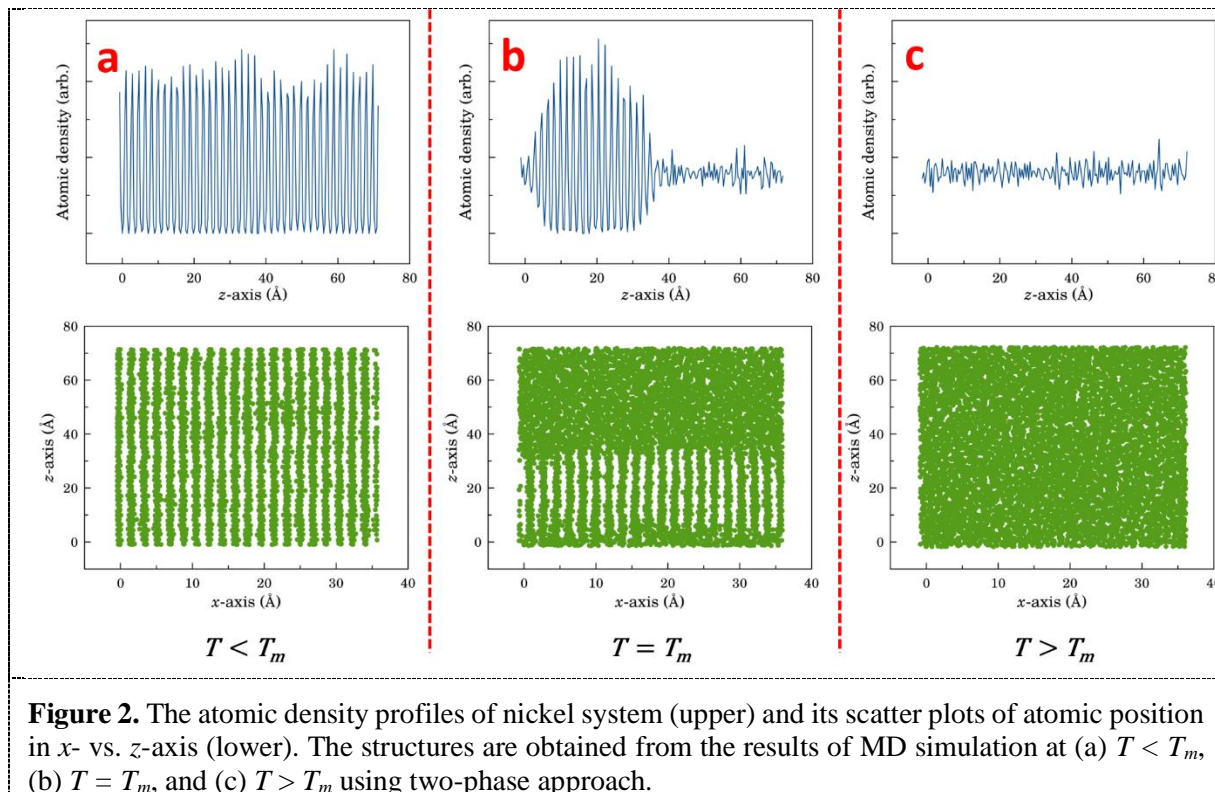


Figure 2 shows the atomic density profile and the scatter plots of the atomic position in  $x$ - vs.  $z$ - axis. The density profile and the scatter plot of the nickel atoms at the temperature  $T$  of the system below the melting temperature  $T_m$  are found in figure 1a. It is clearly shown that the structure is in the regular arrangement indicating the that the recrystallization occurs in this temperature. When the MD simulation are performed at the melting temperature ( $T = T_m$ ) as it appears in figure 1b, the liquid part induce the melting of some atoms in the crystalline part. In this figure, the atoms around the crystalline boundary transform into the liquid structure. It can be seen in figure 1c that the all the nickel atoms change into the liquid structure when the temperature of the system is higher than the melting point ( $T > T_m$ ). In this condition, the atomic structure is completely disordered.

**Table 1.** The melting temperatures of nickel, titanium, and NiTi alloys obtained from the experimental data and from this MD simulation by employing MEAM and EAM potentials.

	Melting Temperature $T_m$ (K)			Accuracy (%)	
	Experiment <sup>a</sup>	MEAM <sup>b</sup>	EAM <sup>b</sup>	MEAM	EAM
Ni	1728	1900 ± 25	1525 ± 25	90.04 %	88.25 %
Ti	1943	1725 ± 25	1550 ± 25	88.78 %	79.77 %
NiTi	1583	2200 ± 25	1500 ± 25	61.02 %	94.76 %

<sup>a</sup> from ref. [22, 23].

<sup>b</sup> This work.

The melting point of nickel, titanium, and NiTi alloy from experimental data and our calculated results are presented in table 1. The calculated melting temperature of nickel, titanium, and NiTi alloy using MEAM potential are around 1900 K, 1725 K, and 2200 K, respectively. The results of nickel and NiTi alloy system overestimate the experimental values [22,23], while the calculated melting point of titanium below the experimental value [22,23]. When the EAM potential is employed in the simulation,

nickel crystal melt at 1525 K and titanium crystal change to the liquid at 1550 K. The NiTi alloy melt at 1500 K when using the EAM potential. All the results of EAM potential are lower than the experimental values [22,23]. It also can be seen in table 1 that the results of MEAM potential exhibit much better accuracy for the system with one species of atom. However, the accuracy of EAM potential is better than the MEAM potential for the alloy system. These results show that the EAM potential outperforms the MEAM potential at high temperature simulation of NiTi alloy, in particular around the melting temperature. It is also shown in our previous simulations that the EAM-type potentials for Al and FeCu alloy give the acceptable performance at high temperature condition [18,24].

### 3.2. Atomic structures in the melting temperature

In this subsection, we show the composition of the atomic structure of the nickel, titanium, and NiTi alloy at their calculated melting temperatures. This information is important to understand the behavior of the melting process for each system.

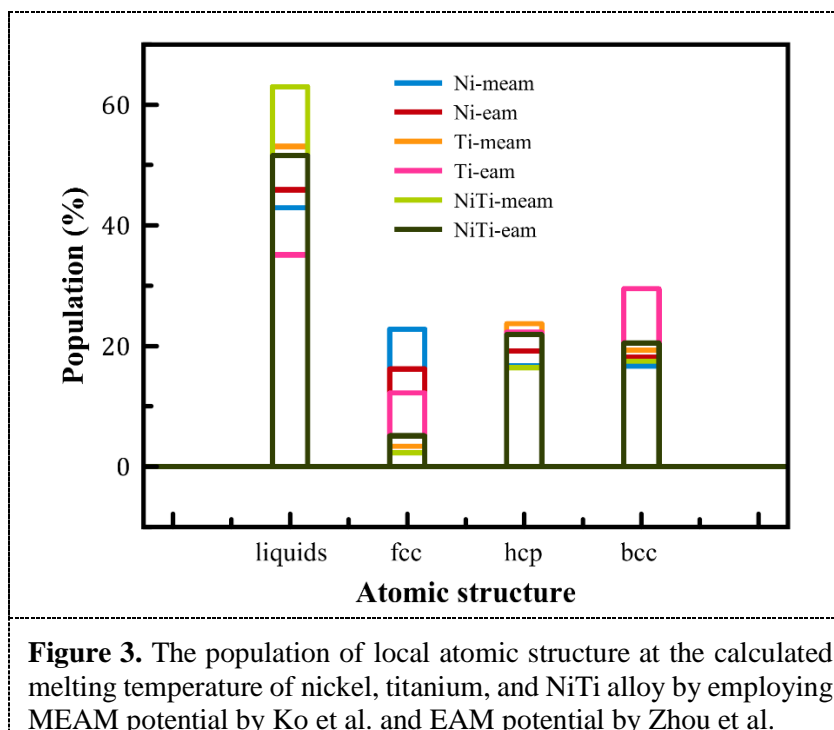


Figure 3 shows the population of the atomic structure at the calculated melting temperature of nickel, titanium, and NiTi alloy using MEAM and EAM potential. It can be seen from figure 3 that in all simulation system, the population of the atomic structures are dominated by the liquids by more than 50 percent. The small population of the original crystalline structure of the system is still found. Some other crystalline structure are also formed in this condition. From these results, we know that the single crystal structure of nickel, titanium, and NiTi alloy will form some other crystal structure before they transform into the liquids structure.

## 4. Conclusion

We have evaluated the performance of the MEAM potential by Ko et al. and the EAM potential by Zhou et al. for nickel, titanium, and NiTi alloy system at high temperature MD simulations. We have obtained the calculated melting temperatures in those simulation systems using two-phase method. In this simulation, the accuracy of MEAM is slightly better than the EAM potential for the nickel and titanium system. The accuracy as high as 94.76 % for NiTi alloy system can be achieved by implementing the EAM potential, while the MEAM potential gives only 61.02 % of accuracy. These result shows that the EAM potential by Zhou et al. outperforms the MEAM potential by Ko et al. for high temperature

simulation of NiTi alloy. Further, we also investigate the atomic structure of the nickel, titanium, and NiTi alloy at the melting temperature. We found in all system that the liquid dominates the structures composition by more than 50 %. It can also be seen that some types of the crystal structures are formed before the atoms melt.

### Acknowledgments

The authors gratefully acknowledge the financial support from DRPM-DIKTI under the PDUPT scheme in fiscal year 2018 with the contract No. 037/SP2H/LT/K7/KM/2018. The contribution of LIPI high performance computing facilities to the results of this research is also acknowledged.

### References

- [1] Saitoh K, Sato T and Sinke N 2006 *Mater. Trans.* **47** 742.
- [2] Jani J M, Leary M, Subic A and Gibson M A 2014 *Mater. Design* **56** 1078.
- [3] Chu C L, Chung C Y, Lin P H and Wang S D 2004 *Mater. Sci. Eng. A* **A366** 114.
- [4] Es-Souni M, Es-Souni M and Brandies H F 2005 *Anal. Bioanal. Chem.* **381** 557.
- [5] Rokicki R, Hryniewicz T, Pulletikurthi C, Rokosz K and Munroe N 2014 *J. Mater. Eng. Performance* **24** 1634.
- [6] Yakubovich A V, Verkhovstev A V, Hanauske M and Solov'yov A V 2013 *Comput. Mater. Sci.* **76** 60.
- [7] Li Y, Li J H and Li B X 2015 *Phys. Chem. Chem. Phys.* **17** 27127.
- [8] Zheng Z Y, Hu C E, Cai L C, Chen X R and Jing F Q 2011 *J. Appl. Phys.* **109** 043503.
- [9] Zhou X W, Jhonson R A and Wadley H N G 2004 *Phys. Rev. B* **69** 144113.
- [10] Ko W S, Grabowski B and Neugebauer J 2015 *Phys. Rev. B* **92** 13410.
- [11] Daw M S and Baskes M I 1983 *Phys. Rev. Lett.* **50** 1285.
- [12] Daw M S and Baskes M I 1984 *Phys. Rev. B* **29** 6443.
- [13] Baskes M I 1992 *Phys. Rev. B* **46** 2727.
- [14] Plimpton S 1995 *J. Comput. Phys.* **117** 1.
- [15] Nosé S 1984 *Molec. Phys.* **52** 255.
- [16] Hoover W B 1985 *Phys. Rev. A* **31** 1695.
- [17] Stukowski A 2010 *Modelling Simul. Mater. Sci. Eng.* **18** 015012.
- [18] Arifin R, Munaji, Sudarno and Purwaningroom D L 2016 *Malay. J. App. Sci.* **1** 52.
- [19] Giorgino T 2014 *Comput. Phys. Commun.* **185** 317.
- [20] Ackland G J and Jones A P 2006 *Phys. Rev. B* **73** 054104.
- [21] Munaji, Sudarno, Purwaningroom D L and Arifin R 2017 *IOP Conf. Ser. Mater. Sci. Eng.* **180** 012252.
- [22] Massalski T B, Okamoto H, Subramanian P R and Kacprzak L 1990 *Binnary Alloy Phase Diagrams* (Ohio: ASM International).
- [23] Frenzel J, George E P, Dlouhy A, Somsen Ch, Wagner M F -X, and Eggeler G 2010 *Acta Mater.* **58** 3444.
- [24] Munaji, Buntoro G A, Purniawan A and Arifin R 2018 *Makara J. Sci.* **22** 137.